

Supplementary Information

Synthesis of Random Poly(Hexyl Thiophene-3-Carboxylate) Copolymers via Oxidative Direct Arylation Polymerization (Oxi-DArP)

Nemal S. Gobalasingham, Robert M. Pankow, Barry C. Thompson

Department of Chemistry and Loker Hydrocarbon Research Institute, University of Southern California,
Los Angeles, California 90089-1661, United States

*Email: barrycth@usc.edu

1. NMR Spectra
2. CV Traces
3. UV-Vis Spectra
4. GIXRD Patterns
5. Thin Film Measurements
6. Extracted Data Table
7. References

1. NMR Spectra

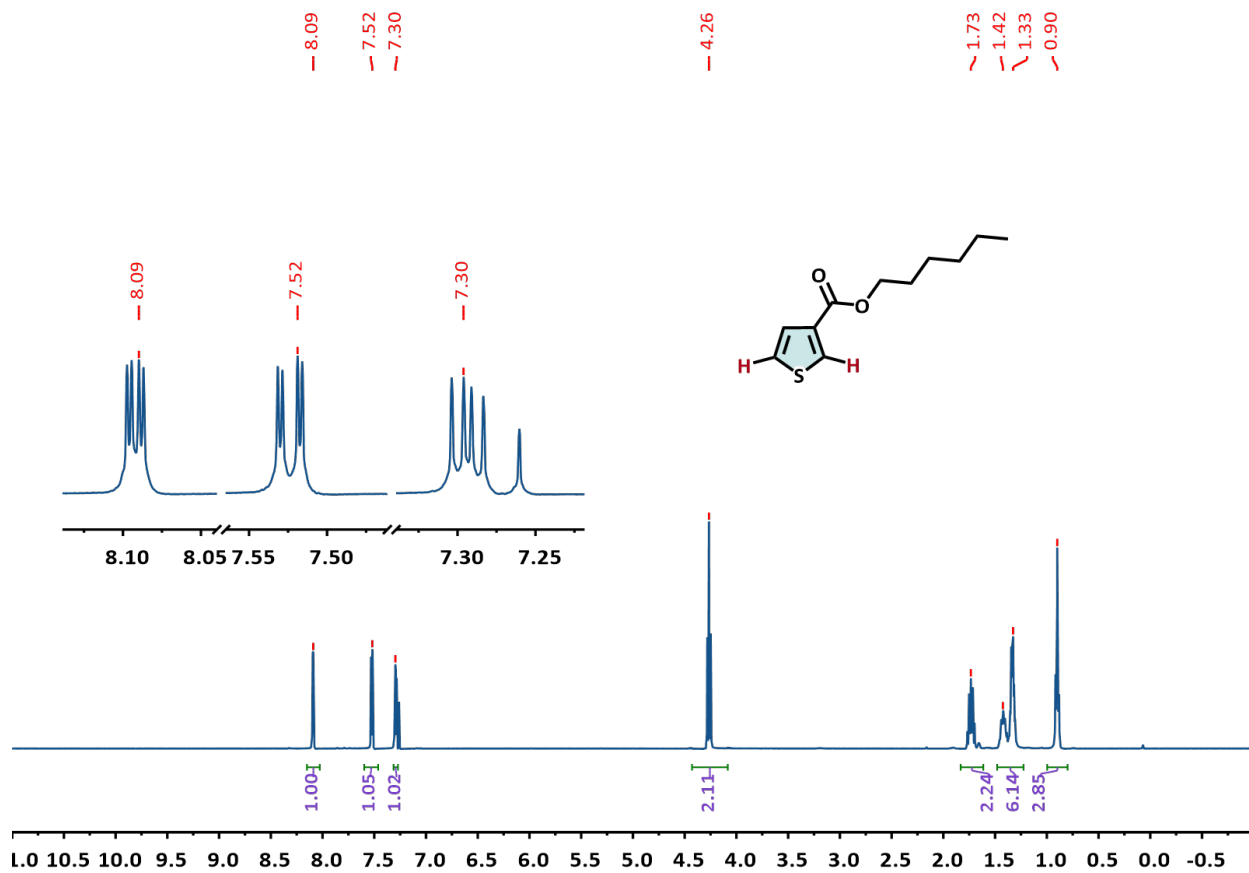


Figure S1. ¹H NMR Spectrum of 3-hexylesterthiophene

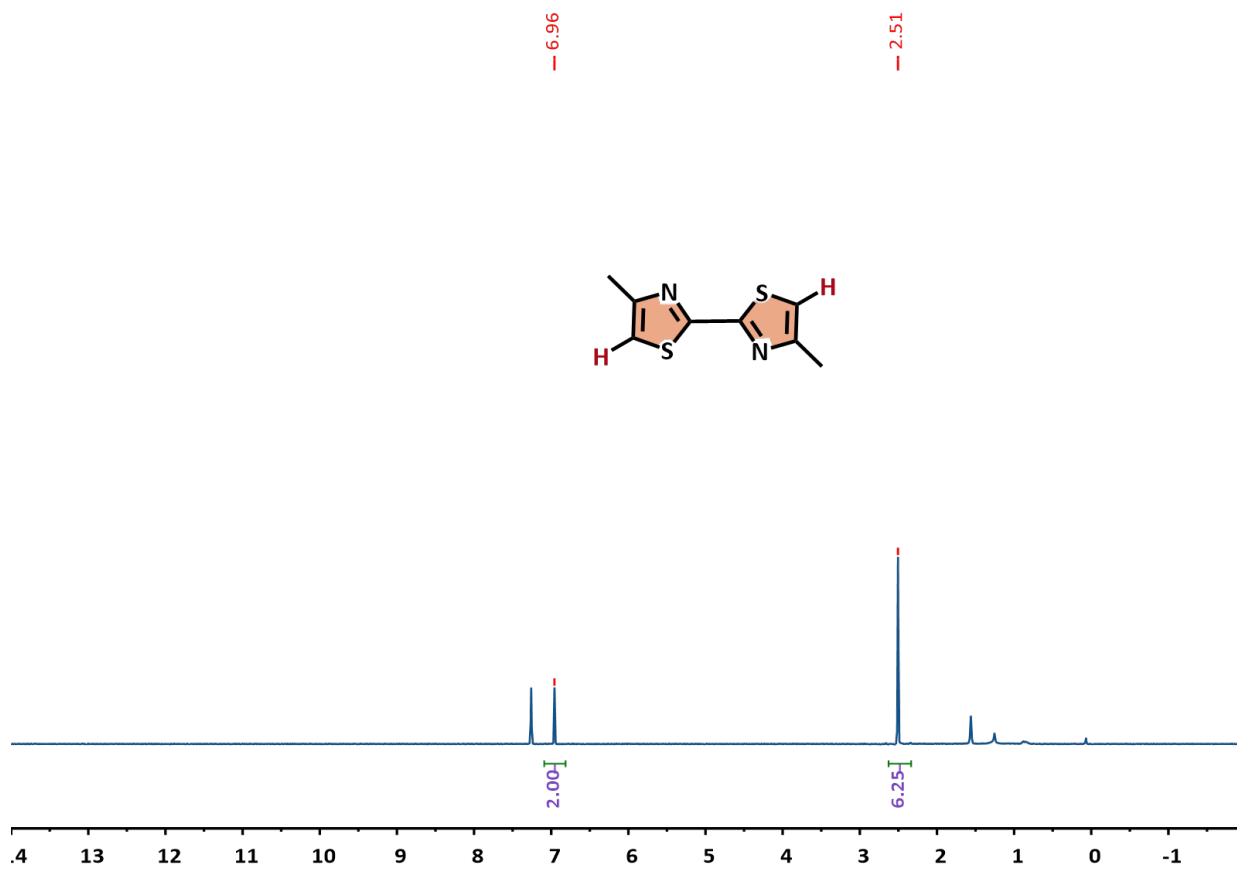


Figure S2. ¹H NMR Spectrum of 4,4'-dimethyl-2,2'-bithiazole (BTz)

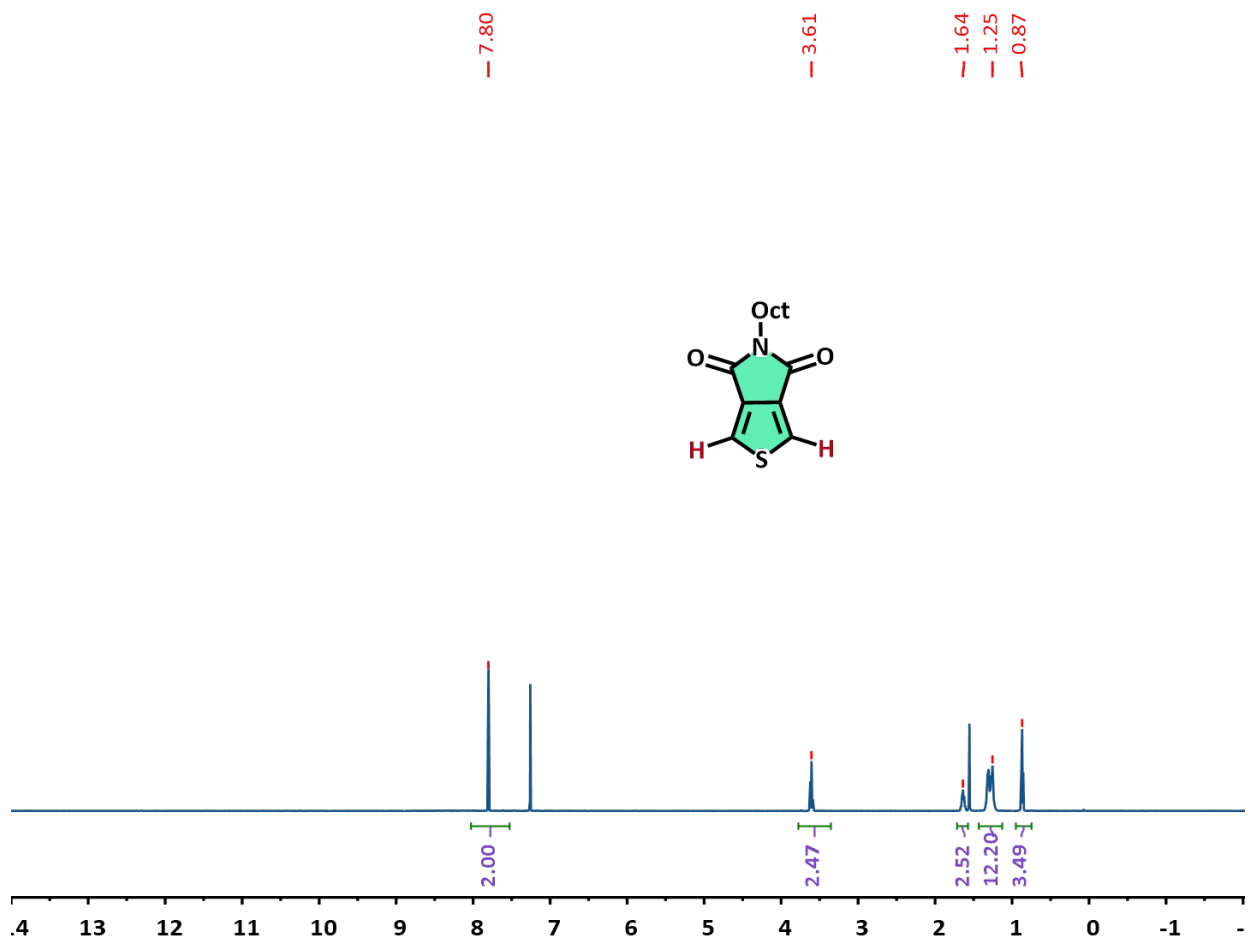


Figure S3. ¹H NMR Spectrum of thieno[3,4-c]pyrrole-4,6-dione (TPD)

P1

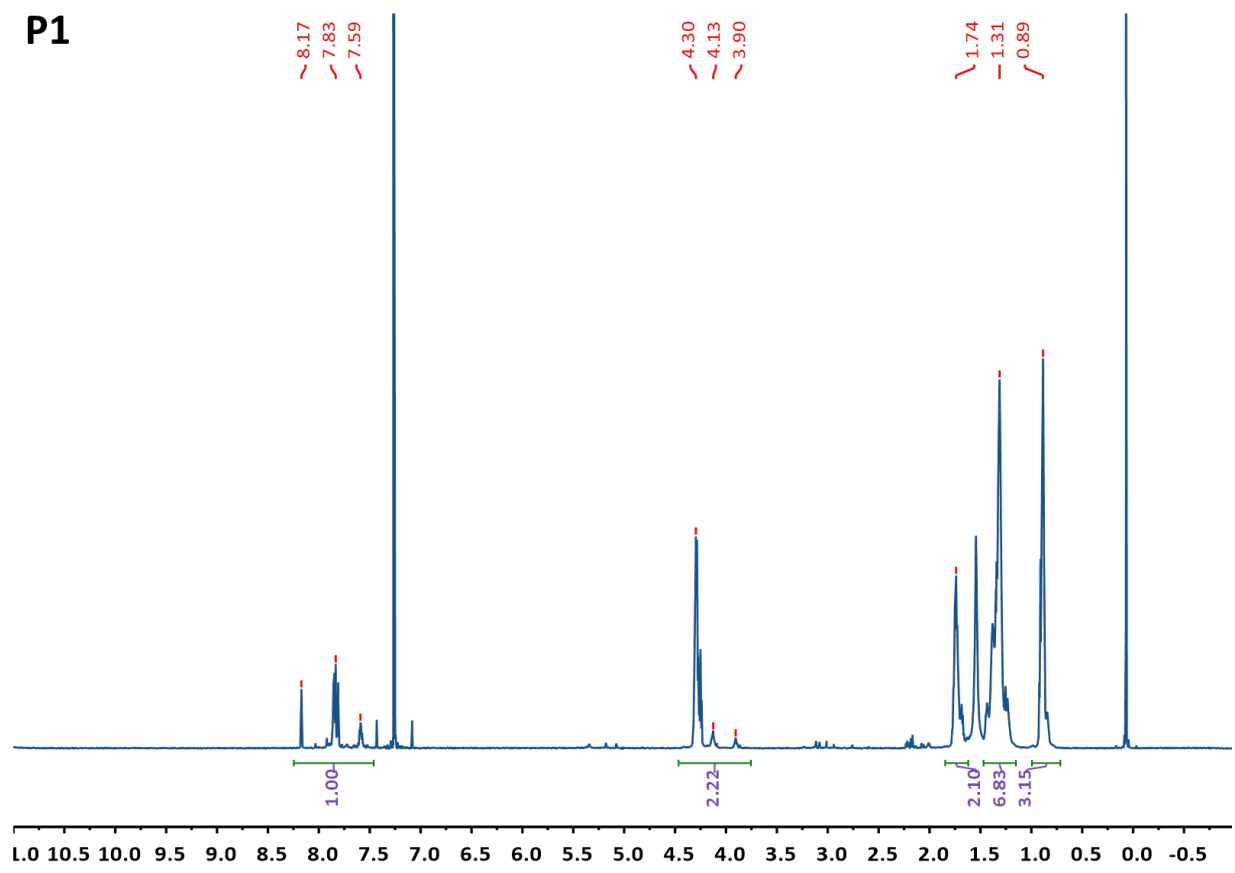


Figure S4. ¹H NMR Spectrum of **P1**

P2

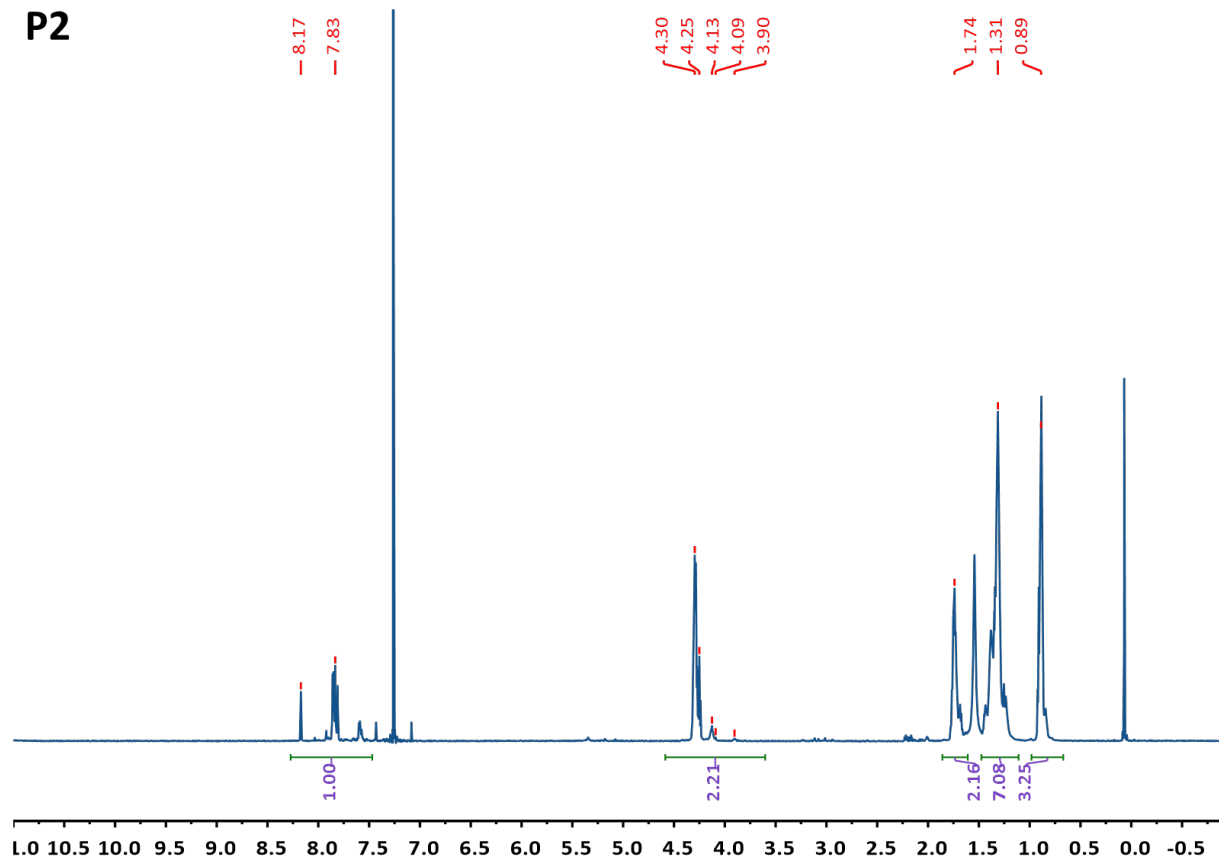


Figure S5. ¹H NMR Spectrum of **P2**

P3

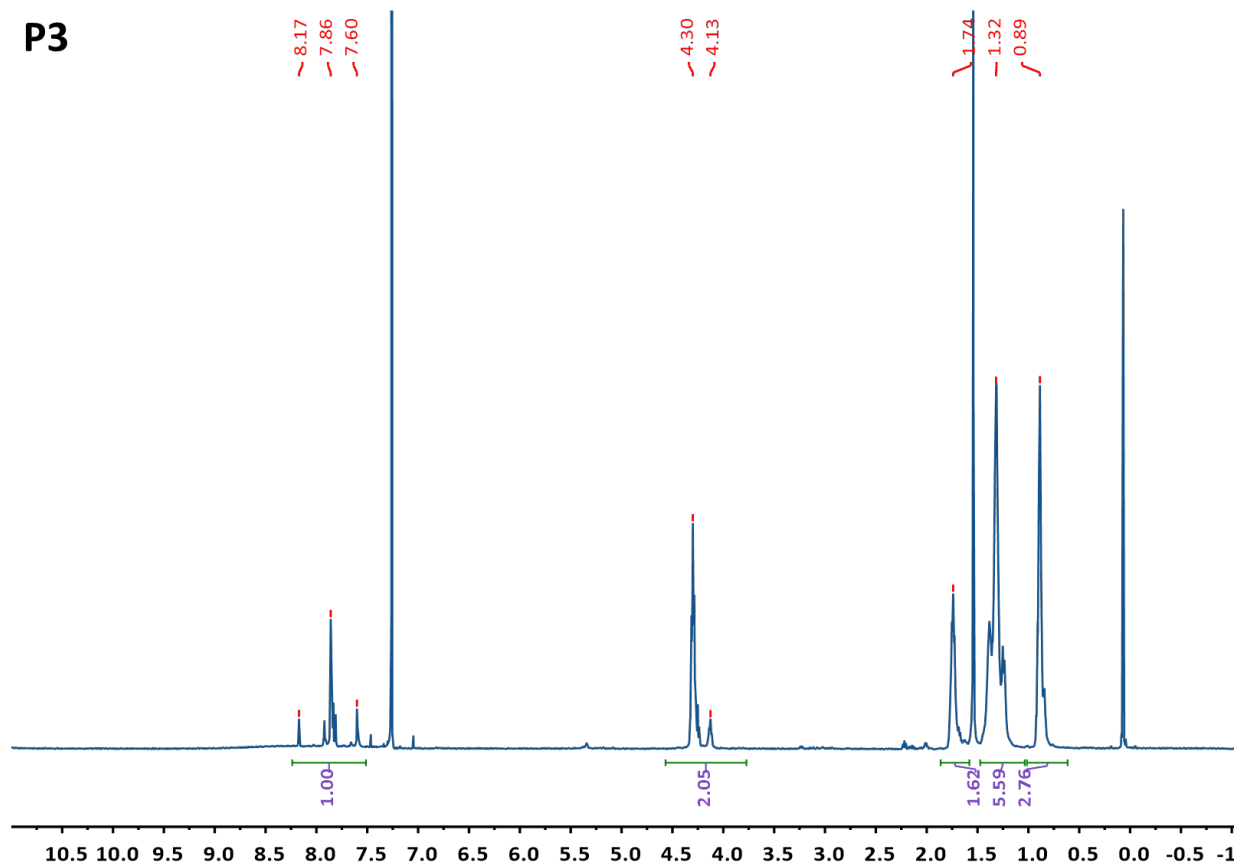


Figure S6. ¹H NMR Spectrum of **P3**

P4

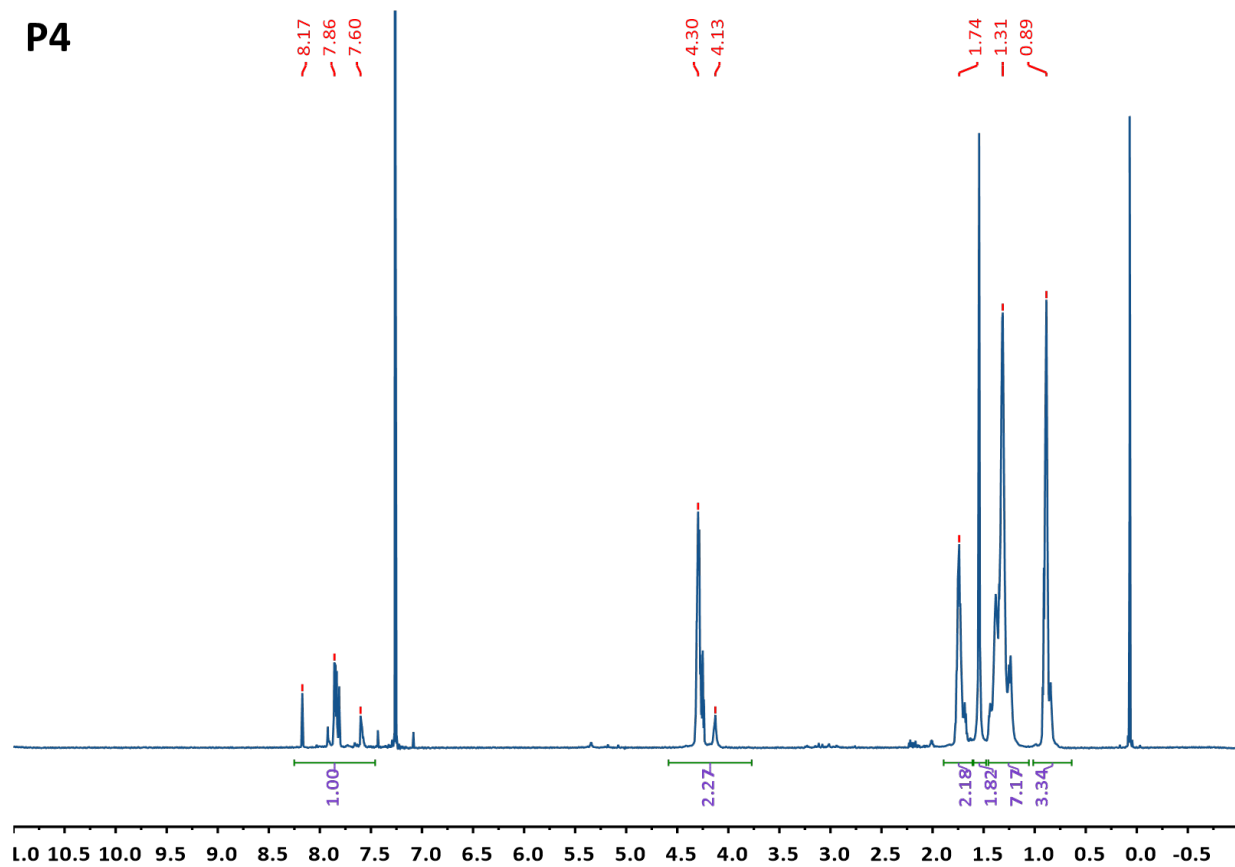


Figure S7. ¹H NMR Spectrum of **P4**

P5

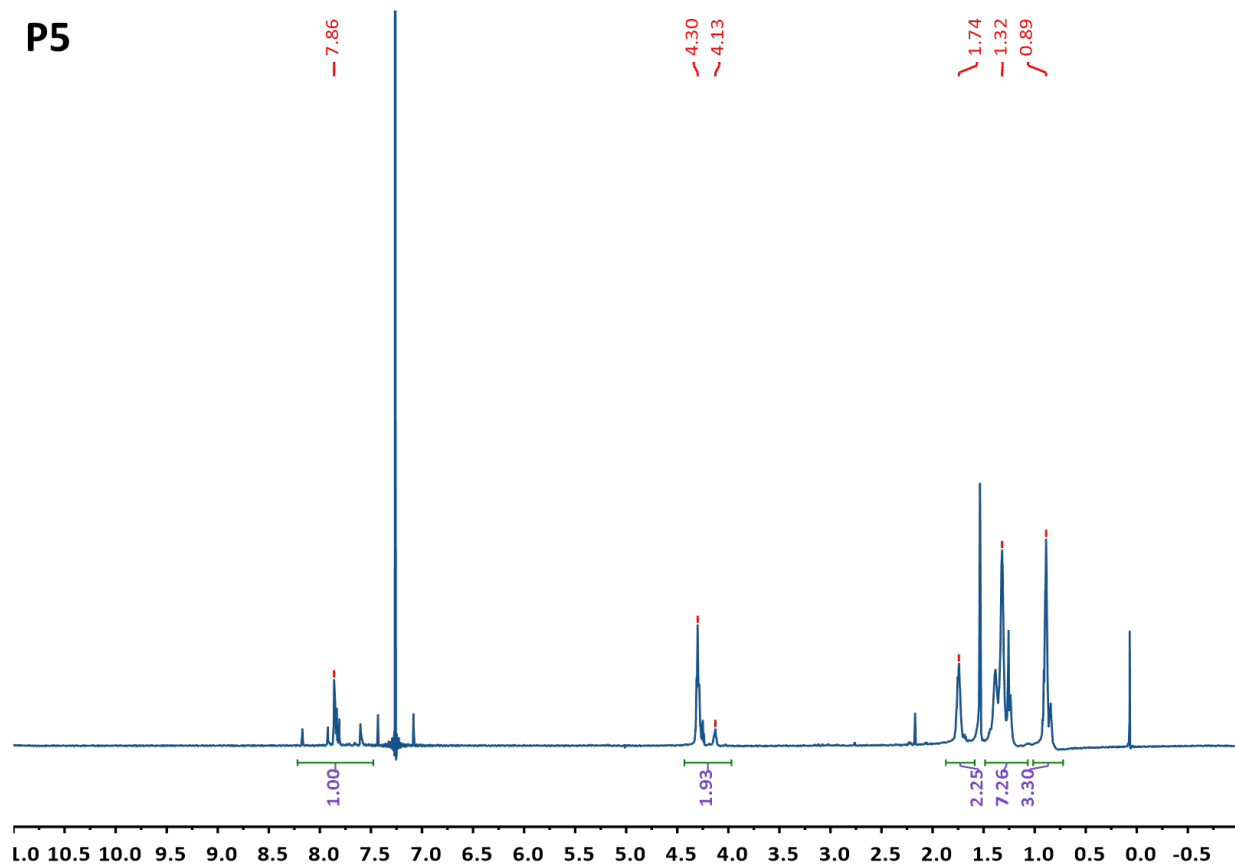


Figure S8. ¹H NMR Spectrum of **P5**

P6

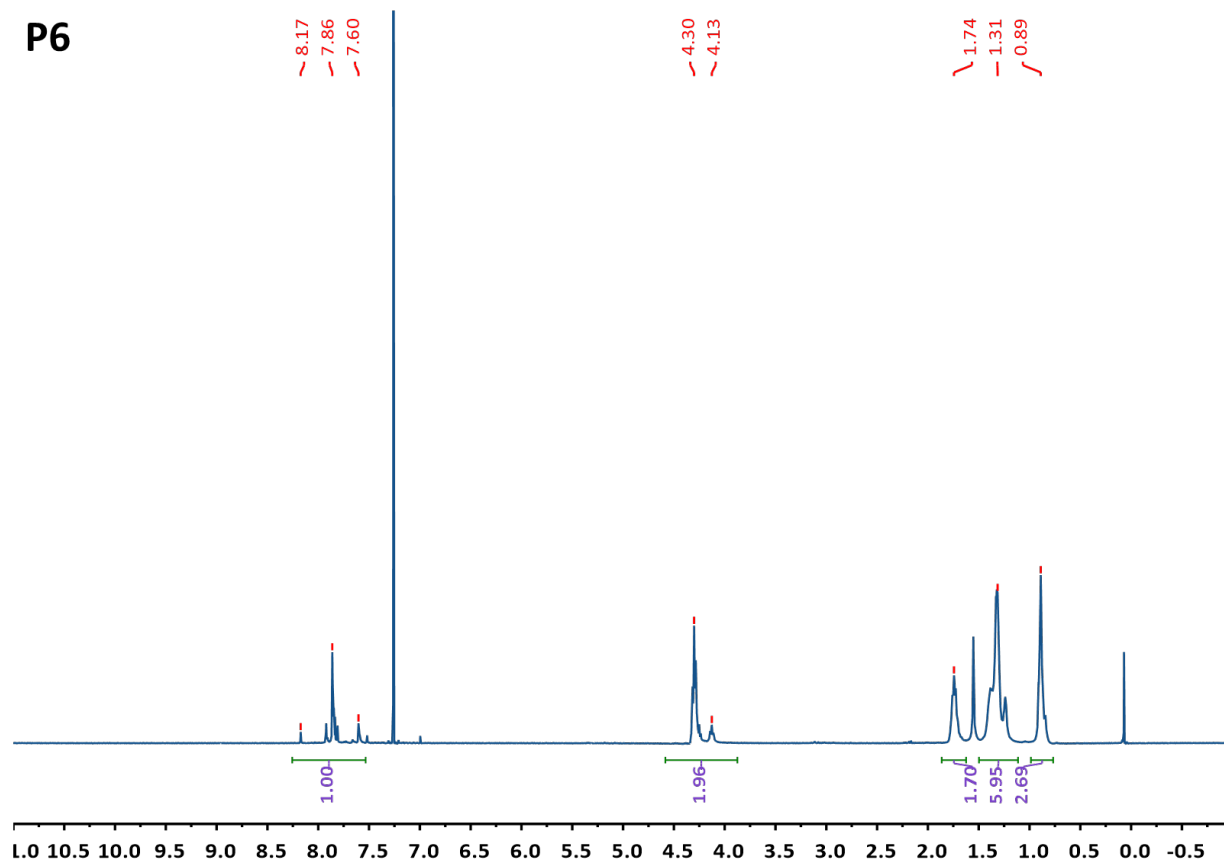


Figure S9. ¹H NMR Spectrum of **P6**

P7

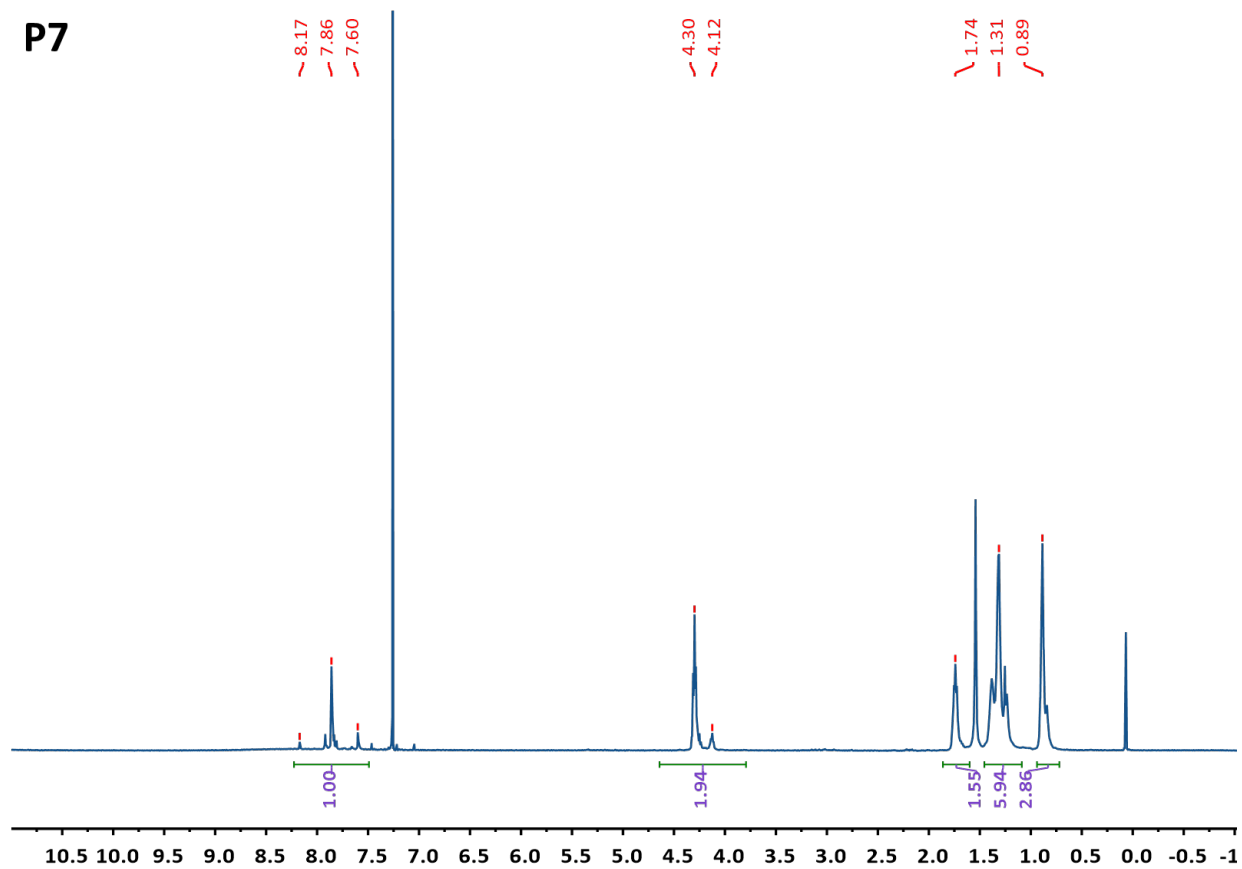


Figure S10. ¹H NMR Spectrum of **P7**

P3HET-BTz-5%

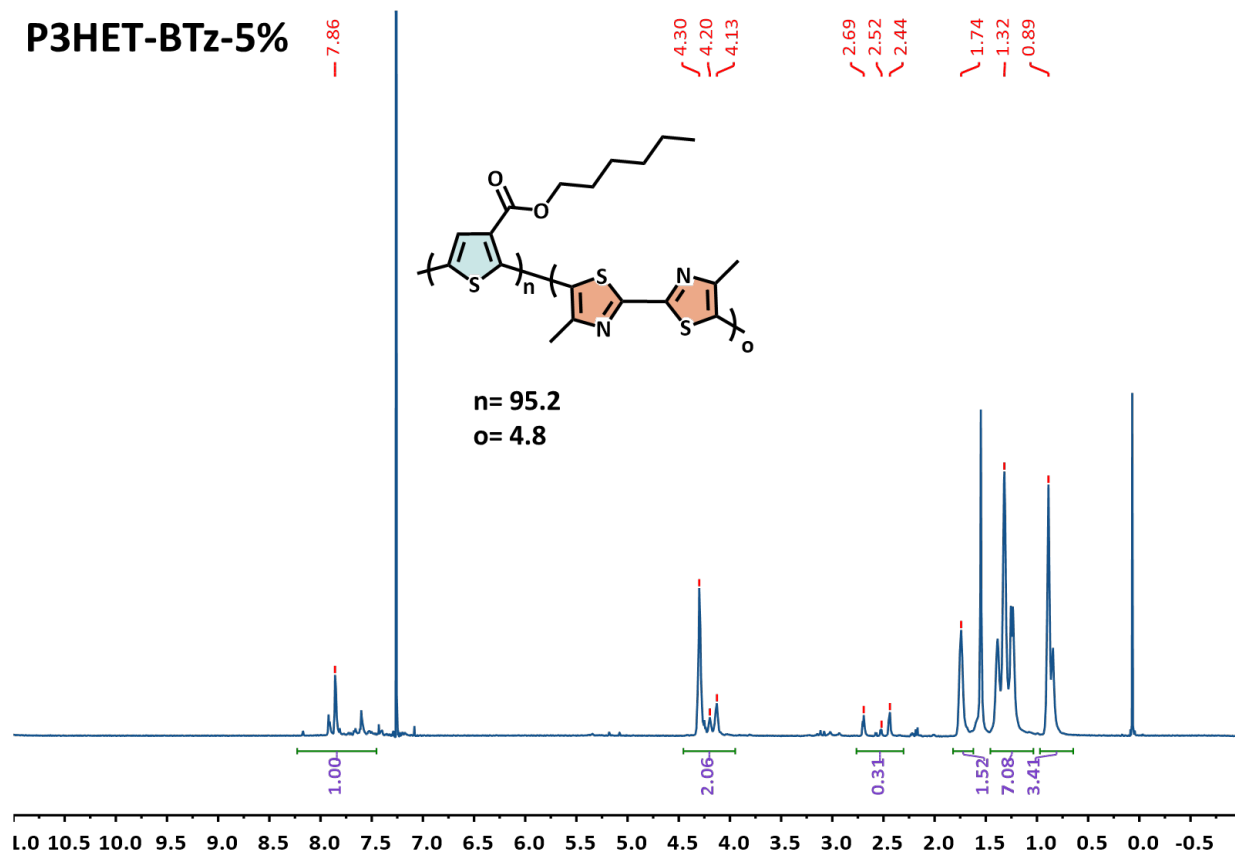


Figure S11. ¹H NMR Spectrum of **P3HET-BTz-5%**

P3HET-BTz-10%

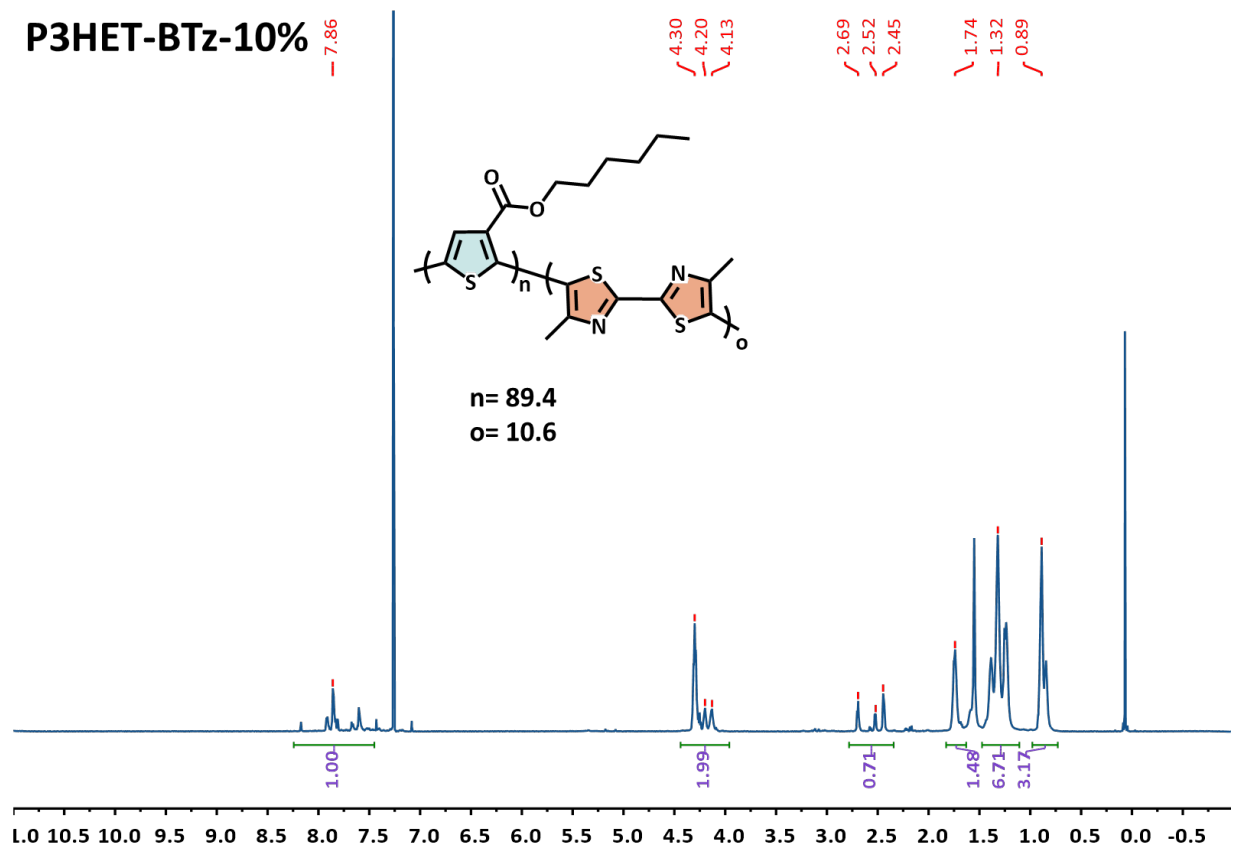


Figure S12. ¹H NMR Spectrum of P3HET-BTz-10%

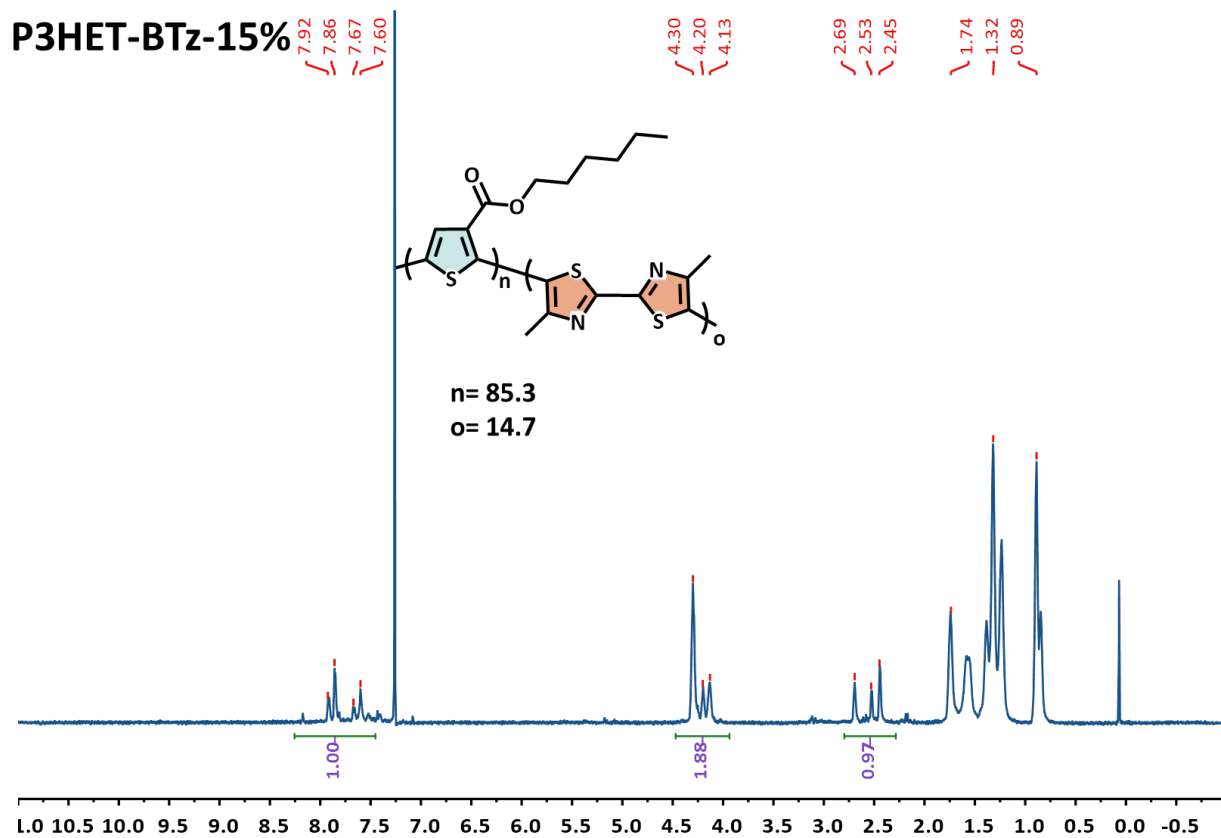


Figure S13. ^1H NMR Spectrum of **P3HET-BTz-15%**

P3HET-TPD-5%

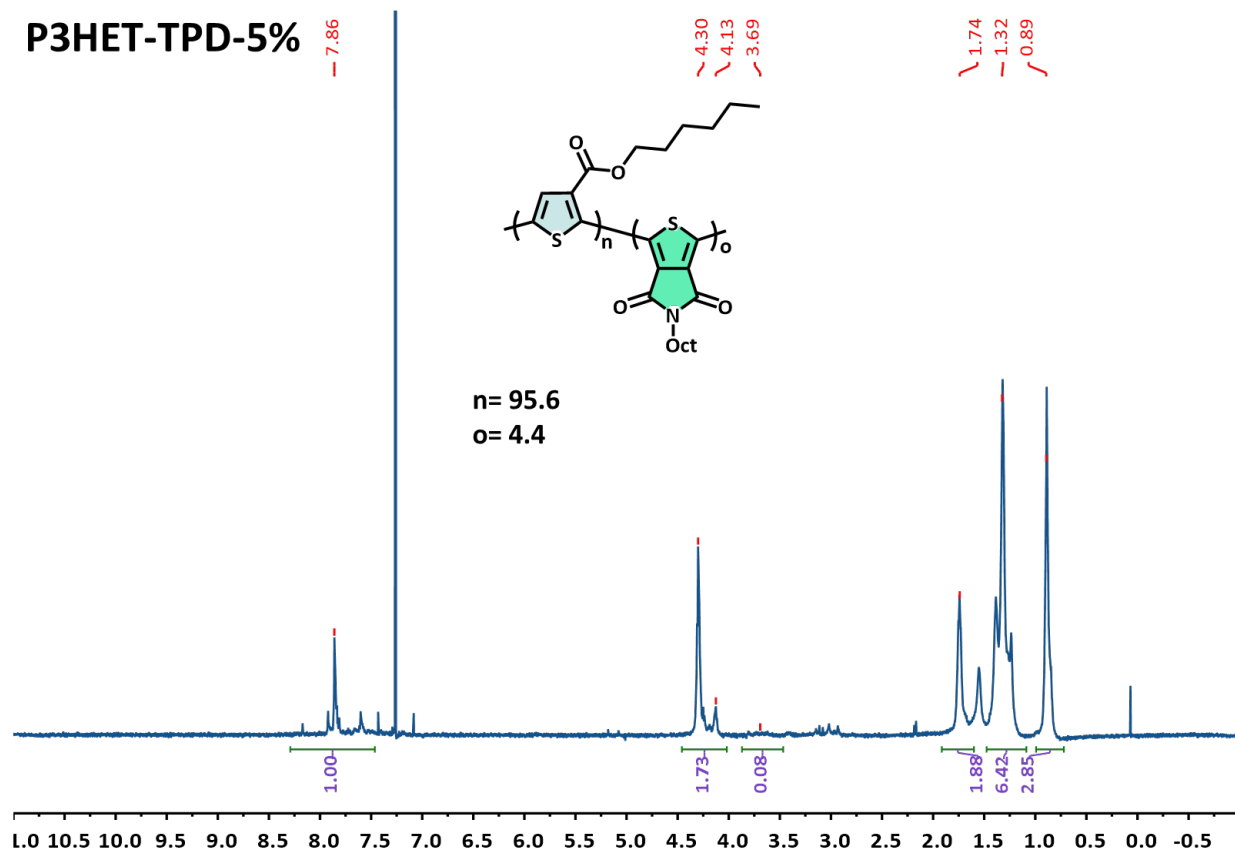


Figure S14. ¹H NMR Spectrum of P3HET-TPD-5%

P3HET-TPD-10%

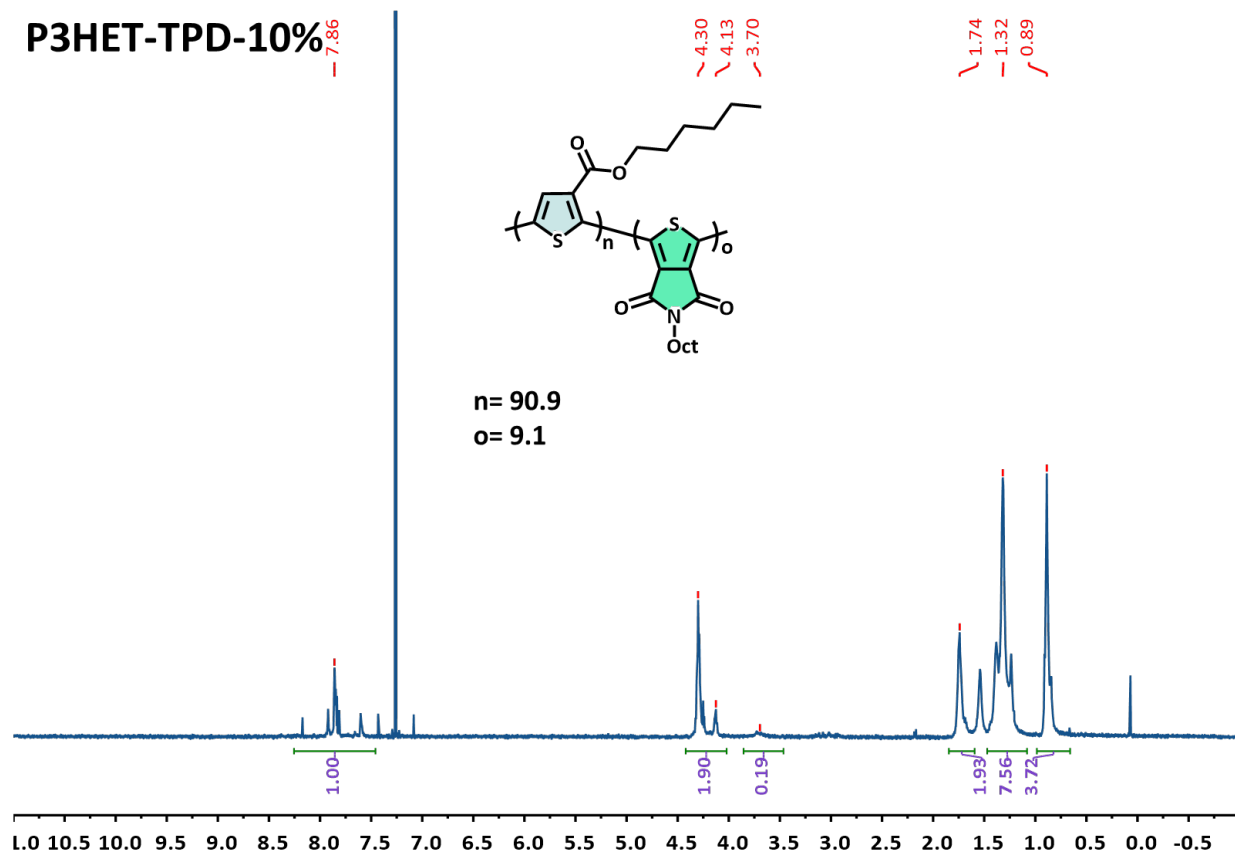


Figure S15. ¹H NMR Spectrum of **P3HET-TPD-10%**

P3HET-TPD-15%

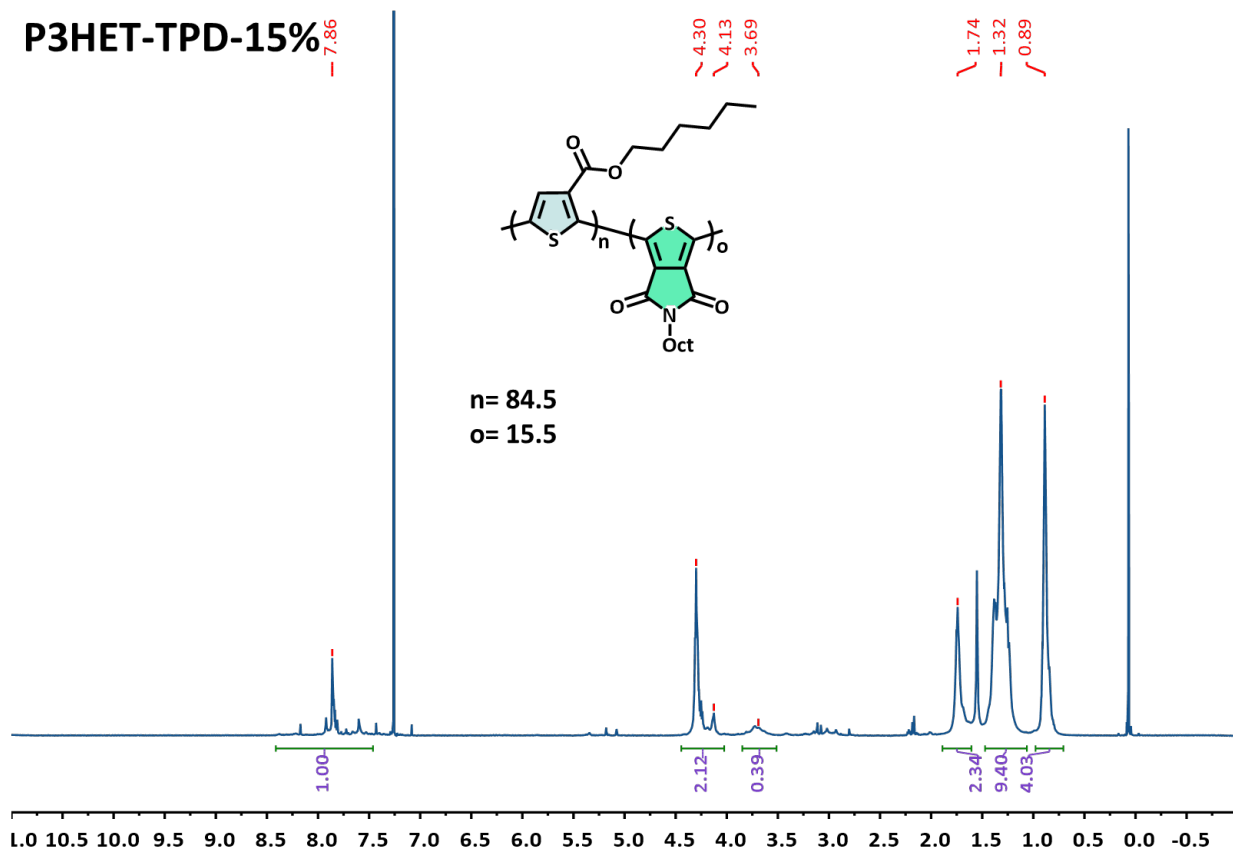


Figure S16. ¹H NMR Spectrum of **P3HET-TPD-15%**

2. CV Traces

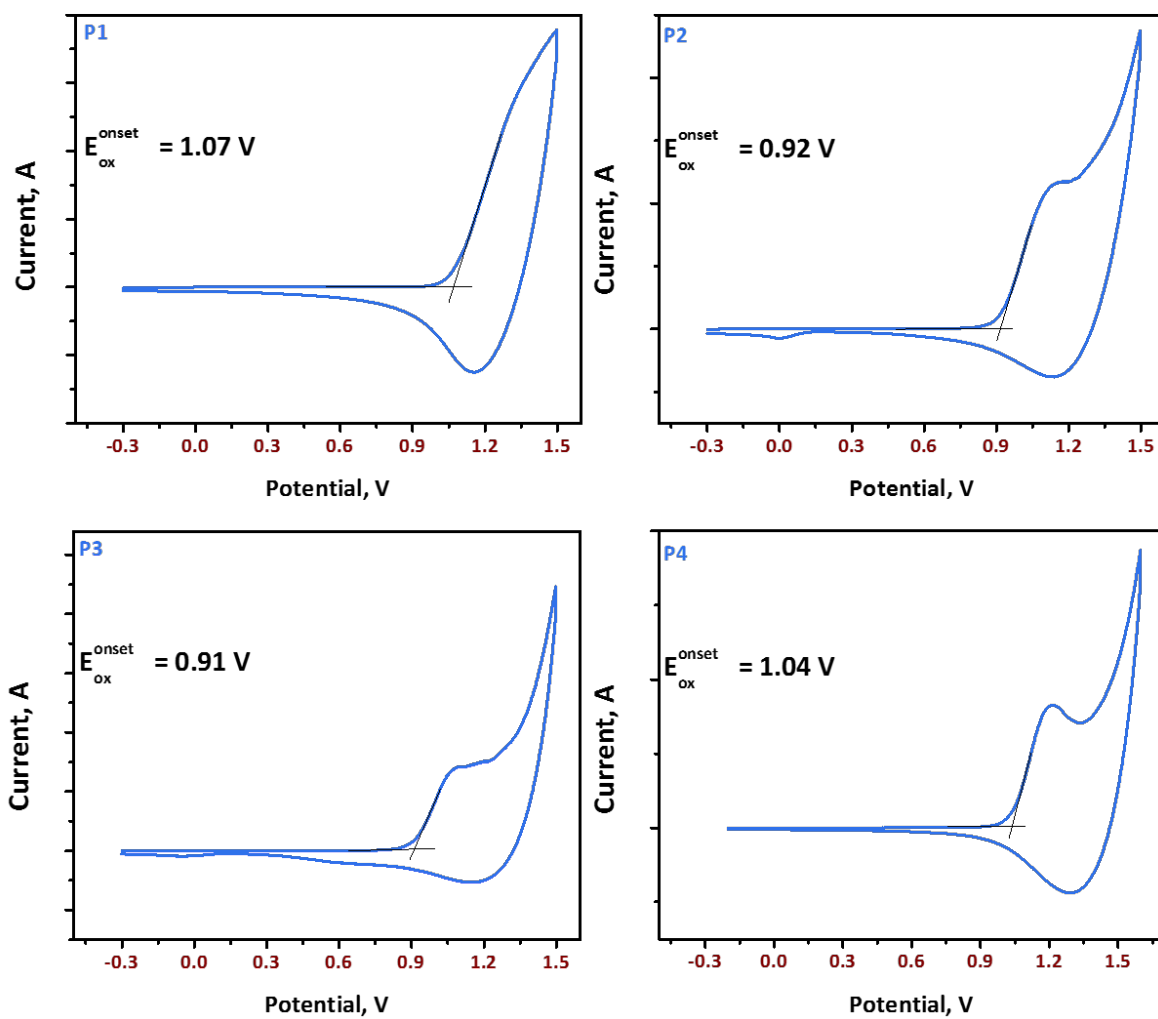


Figure S17. CV Traces for P1-P4

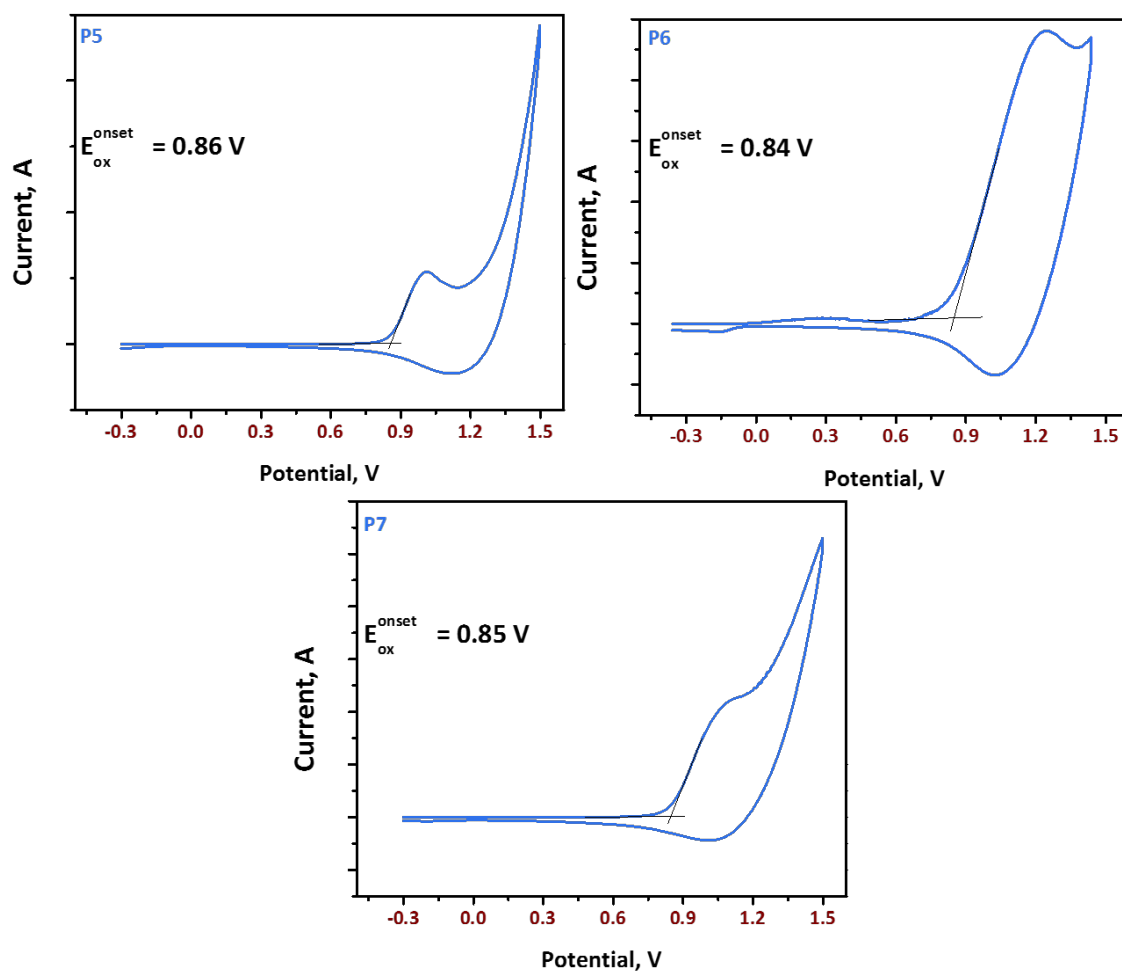


Figure S18. CV Traces for P5-P7

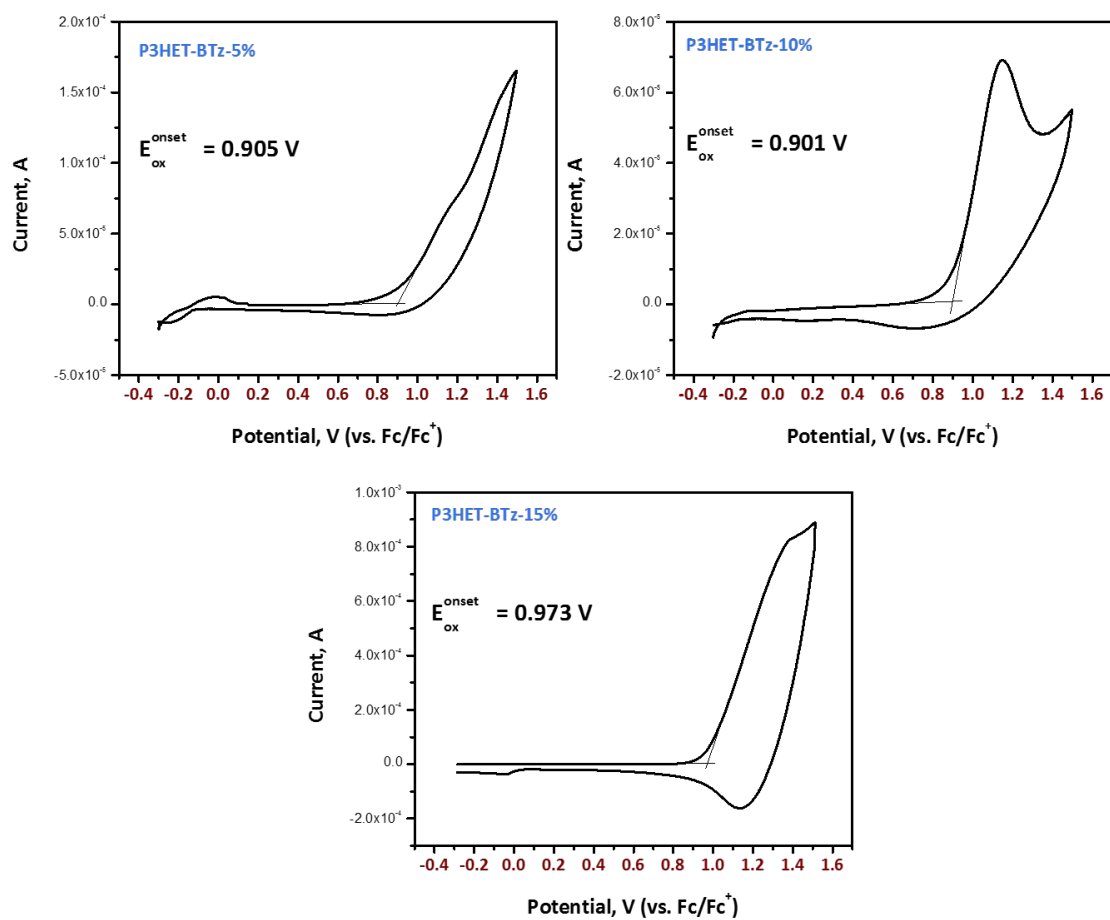


Figure S19. CV Traces of P3HET-BTz Random Copolymers

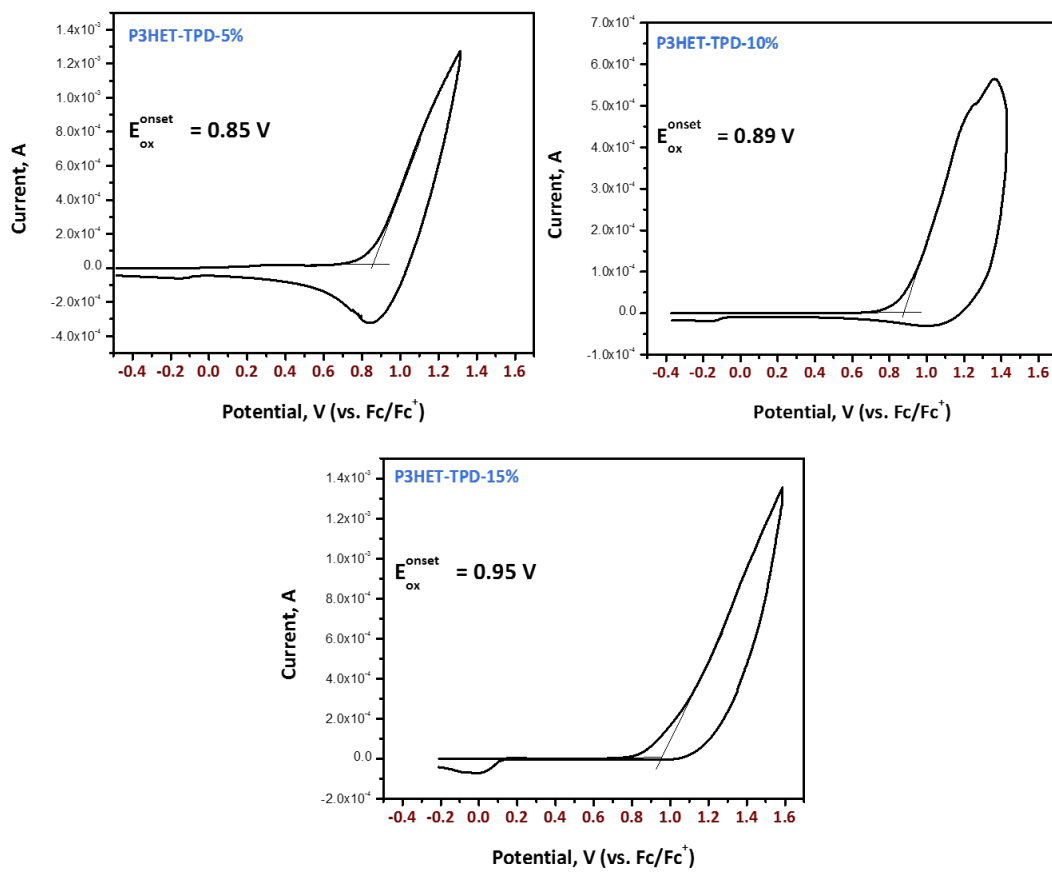


Figure S20. CV Traces of P3HET-TPD Random Copolymers

3. UV-Vis Spectra

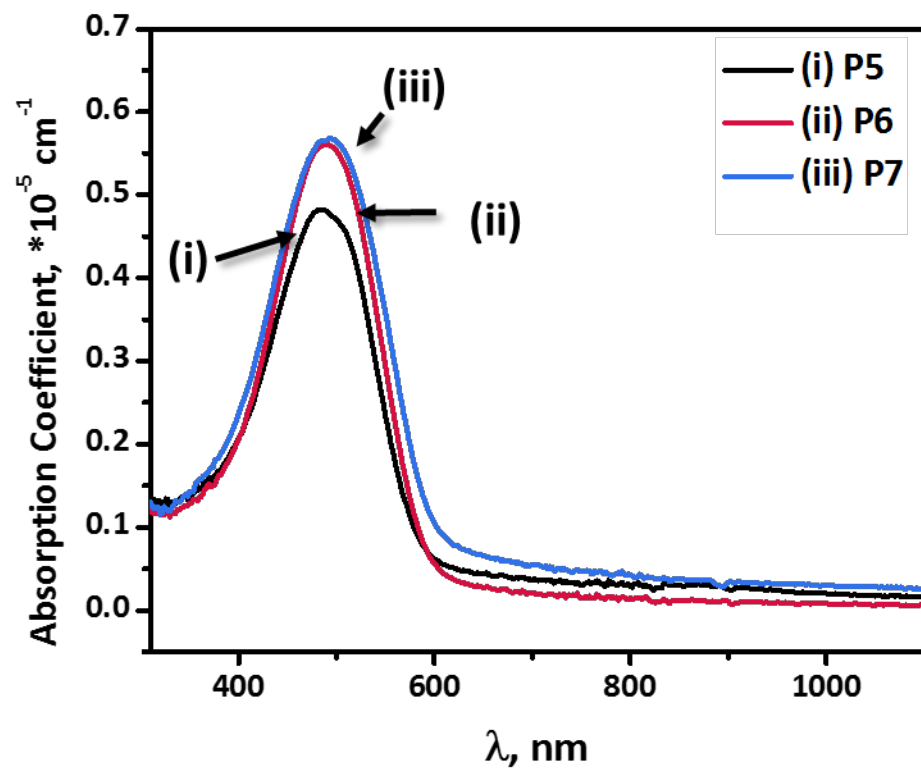


Figure S21. UV-Vis of P5, P6, and P7.

4. GIXRD Patterns

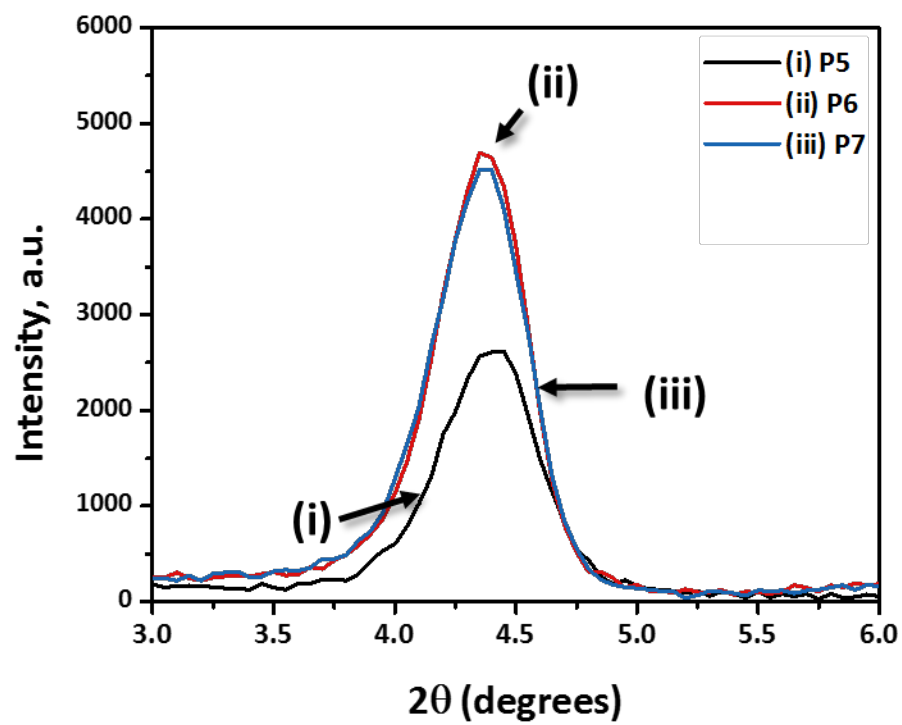


Figure S22. GIXRD Patterns of P5, P6, and P7.

5. Thin Film Measurements.

For thin film measurements, solutions were spin-coated onto pre-cleaned 2.5 cm² glass slides (sonicated for 10 minutes in water, acetone, and isopropyl alcohol then dried under high N₂ flow) from o-dichlorobenzene solutions. The thickness of films and GIXRD measurements were obtained using Rigaku Diffractometer Ultima IV using Cu K α radiation source ($\lambda = 1.54 \text{ \AA}$) in the reflectivity and grazing-incidence X-ray diffraction mode, respectively.

Crystallite size was estimated using Scherrer's equation^{1,2}:

$$\tau = K\lambda/(\beta \cos\theta) \quad (1)$$

where τ is the mean size of the ordered domains, K is the dimensionless shape factor ($K = 0.9$), λ is the x-ray wavelength, β is the line broadening at half the maximum intensity (FWHM) in radians, and θ is the Bragg angle.

Mobility was measured using a hole-only device configuration of ITO/PEDOT:PSS/Polymer/Al in the space charge limited current regime (SCLC).³ The devices preparations for a hole-only device were the same as described below for solar cells. The dark current was measured under ambient conditions. At sufficient potential the mobilities of charges in the device can be determined by fitting the dark current to the model of SCL current and described by equation 2:

$$J_{SCLC} = \frac{9}{8} \epsilon_R \epsilon_0 \mu \frac{V^2}{L^3} \quad (2),$$

where J_{SCLC} is the current density, ϵ_0 is the permittivity of space, ϵ_R is the dielectric constant of the polymer (assumed to be 3), μ is the zero-field mobility of the majority charge carriers, V is the effective voltage across the device ($V = V_{\text{applied}} - V_{\text{bi}} - V_r$), and L is the polymer layer thickness. The series and contact resistance of the hole-only device (18 – 23 Ω) was measured using a blank (ITO/PEDOT/Al) configuration and the voltage drop due to this resistance (V_r) was subtracted from the applied voltage.

The built-in voltage (V_{bi}), which is based on the relative work function difference of the two electrodes, was also subtracted from the applied voltage. The built-in voltage can be determined from the transition between the ohmic region and the SCL region and is found to be about 1 V.

Polymer film thicknesses were measured using GIXRD in the reflectivity mode. Reflectivity profiles are provided below in Figure S23. The spacing between the Kiessig fringes is linked to film thickness. ^{4,5}

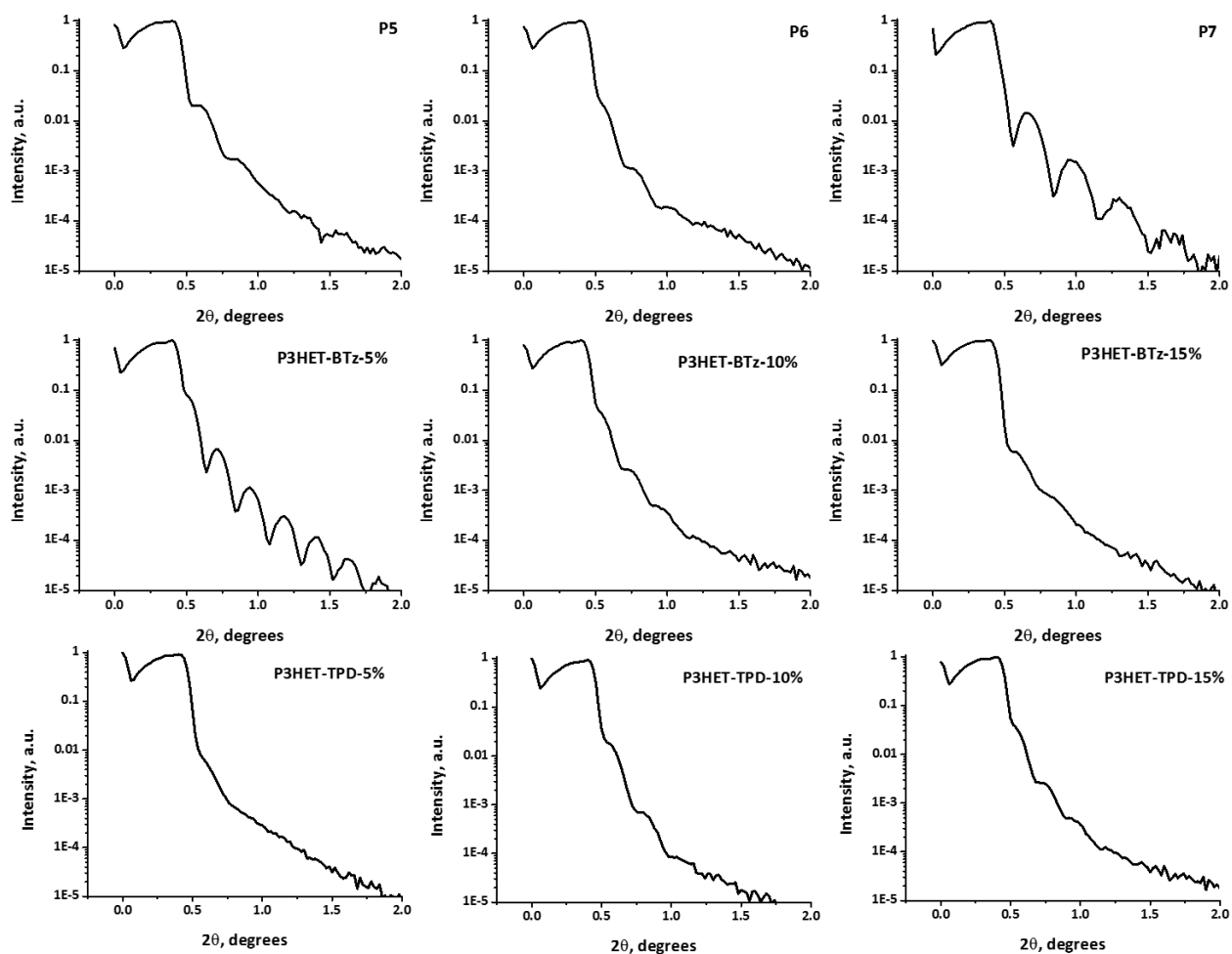


Figure S23. X-ray reflectivity profiles of samples in thin films spin-coated from o-DCB. The spacing between the Kiessig fringes is linked to film thickness, while response from the background determines film roughness. ^{4,5}

6. Data Table

Table S1. Data Table of electrochemical oxidative HOMO levels, peak absorption, peak absorption coefficient, optical bandgaps, 2 θ , GIXRD reflection intensity, d₁₀₀ spacing, full width at half the maximum (FWHM), and crystallite size as estimated from Scherrer's equation for P5, P6, P7, P3HET-BTz Family, and P3HET-TPD Family Polymers

Polymer	HOMO (eV)	$\lambda_{\text{max,abs}}$ (nm)	Film Thickness (nm)	Absorption Coefficient (cm ⁻¹)	E _g (eV)	2 θ (deg)	Intensity (a.u.)	d (Å)	FWHM (deg.)	Crystallite Size (nm)
P5	5.96	483	29.9	48368	2.13	4.43	2653	19.92	0.48	16.59
P6	5.94	488	27.4	56314	2.09	4.36	4720	20.24	0.45	17.70
P7	5.95	494	30.2	57008	2.08	4.37	4542	20.20	0.46	17.31
P3HET-BTz-5%	6.01	488	30.6	59572	2.06	4.54	1604	19.44	0.53	15.03
P3HET-BTz-10%	6.00	480	26.7	61152	2.08	4.7	2339	18.78	0.47	16.95
P3HET-BTz-15%	6.07	467	24.9	48195	2.14	4.8	1351	18.39	0.5	15.94
P3HET-TPD-5%	6.01	495	28.8	61788	2.05	4.29	1968	20.57	0.53	15.03
P3HET-TPD-10%	6.05	494	25.6	59927	2.04	4.14	1255	21.32	0.65	12.25
P3HET-TPD-15%	5.99	491	25.3	55119	2.04	4.09	1684	21.58	0.58	13.73

7. References.

1. H. Yang, S. W. LeFevre, C. Y. Ryu and Z. Bao, *Appl. Phys. Lett.*, 2007, **90**, 172116.
2. A. Sharenko, N. D. Treat, J. A. Love, M. F. Toney, N. Stingelin and T.-Q. Nguyen, *J. Mater. Chem. A*, 2014, **2**, 15717–15721.
3. A. Kokil, K. Yang and J. Kumar, *J. Polym. Sci. B Polym. Phys.*, 2012, **50**, 1130–1144.
4. Kim, H. J. SPIE Newsroom 2009, DOI: 10.1117/2.1200906.16805
5. Kim, H. J.; Lee, H. H.; Kim, J.-J. Proc. of SPIE 2009, 7416, 74160O–9.